Activation and Desensitization of the Recombinant $P2X_1$ Receptor at Nanomolar ATP Concentrations

Jürgen Rettinger and Günther Schmalzing

Department of Molecular Pharmacology, Medical School of the Technical University of Aachen, D-52074 Aachen, Germany

ABSTRACT Activation and desensitization kinetics of the rat $P2X_1$ receptor at nanomolar ATP concentrations were studied in *Xenopus* oocytes using two-electrode voltage-clamp recording. The solution exchange system used allowed complete and reproducible solution exchange in <0.5 s. Sustained exposure to 1–100 nM ATP led to a profound desensitization of $P2X_1$ receptors. At steady-state, desensitization could be described by the Hill equation with a $K_{1/2}$ value of 3.2 ± 0.1 nM. Also, the ATP dependence of peak currents could be described by a Hill equation with an EC_{50} value of 0.7 μM. Accordingly, ATP dose-effect relationships of activation and desensitization practically do not overlap. Recovery from desensitization could be described by a monoexponential function with the time-constant τ = 11.6 ±1.0 min. Current transients at 10–100 nM ATP, which elicited 0.1–8.5% of the maximum response, were compatible with a linear three-state model, *C-O-D* (closed-open-desensitized), with an ATP concentration-dependent activation rate and an ATP concentration-independent (constant) desensitization rate. In the range of 18–300 nM ATP, the total areas under the elicited current transients were equal, suggesting that $P2X_1$ receptor desensitization occurs exclusively via the open conformation. Hence, our results are compatible with a model, according to which $P2X_1$ receptor activation and desensitization follow the same reaction pathway, i.e., without significant *C* to *D* transition. We assume that the $K_{1/2}$ of 3.2 nM for receptor desensitization reflects the nanomolar ATP affinity of the receptor found by others in agonist binding experiments. The high EC_{50} value of 0.7 μM for receptor activation is a consequence of fast desensitization combined with nonsteady-state conditions during recording of peak currents, which are the basis of the dose-response curve. Our results imply that nanomolar extracellular ATP concentrations can obscure $P2X_1$ receptor responses by driving a significant fraction of the receptor pool into a long-lasting refractory closed state.

KEY WORDS: P2X receptor • desensitization • activation

INTRODUCTION

Extracellular ATP excites many neuronal and nonneuronal tissues by activating P2X receptors, which constitute a third major class of ligand-gated ion channels (LGICs)* distinct from the nicotinic acetylcholine receptor (nAChR) superfamily and the glutamate receptor family (North, 1996). The seven known P2X isoforms (designated $P2X_1$ to $P2X_7$) form multiple functional homomultimeric and heteromultimeric channels (Brake et al., 1994; Valera et al., 1994; Bo et al., 1995; Chen et al., 1995; Buell et al., 1996; Collo et al., 1996; Surprenant et al., 1996; Soto et al., 1997). Biochemical and electrophysiological studies have demonstrated that recombinant P2X receptors possess a trimeric architecture in contrast to the canonical pentameric architecture of the nicotinic superfamily members (Nicke et al., 1998, 1999a, 2003; Stoop et al., 1999; Rettinger et al., 2000).

In response to extracellular ATP, P2X receptors open, within milliseconds, an integral ion channel nonselectively permeable to monovalent cations such as Na^+ and K^+ as well as divalent cations such as Ca^{2+} (for reviews see Burnstock, 1999; Mackenzie et al., 1999). Based on their sensitivity to αβ-methylene ATP and rate of desensitization, two P2X receptor phenotypes can be distinguished: (a) $P2X_1$ and $P2X_3$ receptors are αβ-methylene ATP-sensitive and desensitize rapidly in tens or hundreds of milliseconds in the continuous presence of agonist; and (b) $P2X_2$, $P2X_4$, $P2X_5$, and $P2X_7$ receptors are insensitive to αβ-methylene ATP and desensitize only slowly on a timescale of tens of seconds. The different rates of desensitization have been attributed by mutational analysis to various structural motifs, including NH_2- and COOH-terminal domains (Werner et al., 1996; Koshimizu et al., 1999) and a highly conserved protein kinase C site (Boue-Grabot et al., 2000). It should be noted that the term desensitization as used in the present study refers to a reversible functional inactivation by a conformational transition of the LGIC itself rather than to down-regulation by LGIC internalization and related cellular processes, which lead to a reduction of the number of receptor molecules in a given plasma membrane (Ennion and Evans, 2001).

Address correspondence to J. Rettinger, University Medical School, RWTH Aachen, Department of Molecular Pharmacology, Wendlingweg 2, D-52074 Aachen, Germany. Fax (49) 241 8082433; E-mail: jrett@web.de

*Abbreviations used in this paper: LGIC, ligand-gated ion channel; nAChR, nicotinic acetylcholine receptor.

J. Gen. Physiol. © The Rockefeller University Press • 0022-1295/2003/05/451/11 $8.00
Volume 121 May 2003 451–461
http://www.jgp.org/cgi/doi/10.1085/jgp.200208730

The occurrence of fast receptor desensitization in the presence of agonist was first studied in detail for the acetylcholine response at frog muscle end-plates (Katz and Thesleff, 1957). Upon steady application of acetylcholine, the end-plate becames refractory to acetylcholine within seconds; sensitivity recovered slowly after complete removal of acetylcholine. The absence of detectable depolarization during recovery implied a cyclic model for nAChR activation and desensitization with the existence of two distinct conformations in the absence of agonist: a closed resting state, *C*, and a closed desensitized state, *D*, linked by an open state, *O*. If the agonist binds, the nAChR opens and then desensitizes; upon washout, the agonist dissociates and the nAChR returns to its resting condition without reopening. To account for the observation that a given agonist concentration can produce little depolarization, yet lead to pronounced desensitization, it was proposed (Katz and Thesleff, 1957) and later experimentally confirmed (Changeux, 1990) that the unliganded desensitized state of the nAChR features a much higher affinity for the agonist than the resting state. The cyclic reaction scheme predicts that the low affinity resting state *C* can undergo a conformational transition without ligand binding and opening into the high affinity desensitized state *D*. In agreement with this model, ~20% of the total nAChR population exists in the high affinity desensitized state even in the absence of agonist (Changeux, 1990). Consequently, at low acetylcholine concentrations, selective binding to the desensitized nAChRs can occur, thus shifting the equilibrium from the favored low affinity resting state toward the desensitized state. Sustained exposure to low levels of agonists can thus result without activation in the accumulation of a large fraction of receptors in desensitized states and hence reduce neuronal excitability (Dani and Heinemann, 1996). Regular fast receptor activation requires comparably high agonist concentrations that allow for the occupancy of the low affinity resting state of the receptors.

In this study, we used whole-cell current recordings in *Xenopus* oocytes to assess the kinetics of activation and desensitization of the recombinant rat $P2X_1$ receptor. The aim of this study was to examine whether the $P2X_1$ receptor also desensitizes by subthreshold levels of ATP like other LGICs. To this end, we preincubated oocytes expressing the $P2X_1$ receptor under voltage-clamp conditions with submicromolar concentrations of ATP for prolonged times. Our results demonstrate that a 50% steady-state desensitization of the rat $P2X_1$ receptor can be achieved by an ATP concentration as low as 3 nM, which elicits <0.1% of the maximum current recorded at nonpredesensitized $P2X_1$ receptors. These results are discussed in terms of current models describing LGIC activation and desensitization kinetics. A simple kinetic scheme is proposed to account for our data on the $P2X_1$ receptor.

MATERIALS AND METHODS

LGIC Expression in Xenopus Oocytes

Plasmids encoding the wild-type rat $P2X_1$ subunit (EMBL/GenBank/DDBJ accession no. U14414) (Nicke et al., 1998) or the muscle type nAChR (Witzemann et al., 1990; Nicke et al., 1999b) have been described previously. Capped cRNAs were synthesized from linearized templates with SP6 RNA polymerase (Amersham Biosciences), purified by sepharose G50 chromatography and phenol-chloroform extraction, and dissolved in 5 mM Tris/HCl, pH 7.2, at 0.5 μg/μl using the optical density reading at 260 nm for quantitation (OD 1.0 = 40 μg/μl). Follicle cell–free *Xenopus laevis* oocytes were isolated as described previously (Schmalzing et al., 1991) and injected with 50-nl aliquots of cRNA. Until electrophysiological experiments took place, the injected oocytes were incubated at 19°C in sterile oocyte Ringer's solution (ORi: 90 mM NaCl, 1 mM KCl, 1 mM $CaCl_2$, 1 mM $MgCl_2$, and 10 mM HEPES, pH 7.4) supplemented with 50 μg/ml of gentamycin.

Electrophysiology

Whole-cell currents were recorded 2–4 d after cRNA injection using the two-electrode voltage-clamp method. Microelectrodes were prepared from borosilicate glass and filled with 3 M KCl. The tips were broken to achieve electrical resistances below 1.0 or 1.5 MΩ for the current and the potential electrode, respectively. Currents were recorded with a Turbo TEC-05 amplifier (npi electronics), low-pass filtered at 200 Hz, and sampled at 500 Hz (AD/DA-Converter INT-10; npi electronics) using a commercially available software (EggWorks; npi electronics). The holding potential was −60 mV in all experiments. For perfusion of oocytes, a nominally Ca^{2+}-free ORi solution was used (designated Mg-Ori), in which Ca^{2+} was replaced by Mg^{2+} to avoid activation of endogenous Cl^- channels (Methfessel et al., 1986). All measurements were performed at ambient temperature (20–22°C).

Agonist Application

To allow for rapid solution exchange, an oocyte-recording chamber with a small bath volume of ≈10 μl was combined with fast bath perfusion at a constant flow rate of ≈200 μl/s. Solutions were applied by the use of a manifold made of glass capillaries and silicon tubing (Fig. 1 A). Current signals were elicited by switching between ATP-free to ATP-containing Mg-ORi. Switching between solutions was attained by magnetic valves, which enabled computer-controlled applications of solution by using the EggWorks software.

In experiments designed to determine the rate of entry into desensitization at submicromolar ATP concentrations, oocytes were used only once because of the slow recovery from desensitization of the $P2X_1$ receptor. Oocytes were voltage-clamped to −60 mV and then continuously superfused with 3–100 nM ATP in Mg-ORi for different lengths of time (20 s to 20 min). At the end of the predetermined preincubation period, the residual peak current was elicited by application of a saturating test pulse of 30 μM ATP. The fraction of $P2X_1$ receptors in the resting state was then calculated by normalizing the residual peak current to the mean current response to 30 μM ATP recorded at the same day from a subgroup of the same cRNA-injected oocytes that had never been incubated with ATP before. The control responses used for normalization were recorded after preincubation periods in ATP-free Mg-ORI identical in duration to the respective

residual responses. The standard error of means was propagated into error bars of the normalized values using the usual formulas of error propagation.

Data Analysis

Responses were quantified by measuring the peak current amplitude relative to the baseline holding current recorded immediately preceding agonist application. Agonist dose-response curve parameters were determined by nonlinear curve fitting of the Hill equation to the data using Origin software (version 5.0; Microcal Corporation). Data are expressed as mean ± SEM. Further details of data analysis including the equations used are given under RESULTS and in the figure legends.

Computer Simulations

For simulation of reaction schemes and sets of rate constants, the software GEPASI was used (Mendes, 1993, 1997). To obtain ATP-dependent data, the time courses of the receptor currents were calculated with an appropriate set of rate constants. These simulated receptor currents were then analyzed in the same manner as the experimentally determined receptor currents.

RESULTS

Rate of Solution Exchange

The onset of the current of the muscle type nAChR formed by αβγδ nAChR subunits activated by 30 μM acetylcholine has been demonstrated to provide a reliable estimate of the speed of solution exchange around *Xenopus* oocytes (Dilger and Brett, 1990; Costa et al., 1994). By activating oocytes expressing the muscle nAChR (Nicke et al., 1999b) with 5-s acetylcholine pulses (30 μM), a current rise time $t_{10–90\%}$ of ~150 ms was determined for a 10–90% increase of the peak current amplitude. Repetitive activation of the same oocyte in 1-min intervals with acetylcholine generated virtually indistinguishable current traces (Fig. 1 B), thus demonstrating the excellent reproducibility of the solution exchange. For data analysis and kinetic modelling, only time constants were considered that were at least one order of magnitude larger than the $t_{10–90\%}$ value of the solution exchange.

Steady-state Desensitization of the $P2X_1$ Receptor at Submicromolar ATP Concentrations

At the near-saturating micromolar ATP concentrations typically used to activate the $P2X_1$ receptor in electrophysiological experiments, the inward current rises fast to peak and then declines in <1 s, leading to a complete loss of the response in the sustained presence of ATP as a result of receptor desensitization. Since recovery from desensitization occurs at slow rate (τ ~12 min, see next paragraph), a long-lasting desensitized state follows activation by pulse applications of high concentrations of ATP. Even at an ATP concentration as low as 100 nM, which elicits only ~10% of the maximum current response, full desensitization occurs within a few seconds of continuous exposure to ATP, as deduced from the inability of a subsequent application of 30 μM ATP to evoke any current response (compare Fig. 2 B). This raises the question to what extent even smaller ATP concentrations are able to desensitize the $P2X_1$ receptor and at what rate this desensitization occurs.

To address this question, we superfused oocytes under voltage-clamp conditions for different time periods with Mg-ORi containing a defined ATP concentration ranging from 3–100 nM. At a predetermined time

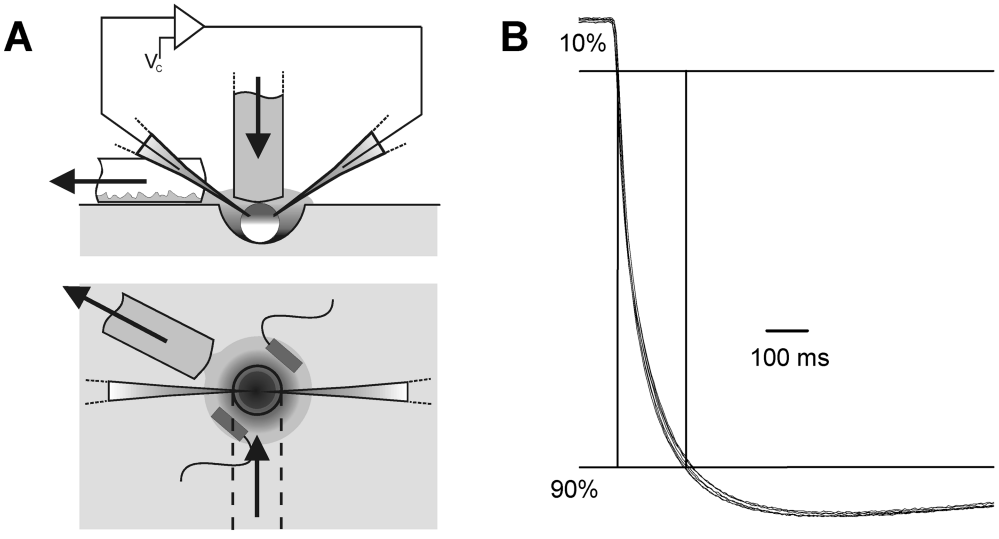

FIGURE 1. Schematic drawing of the fast solution exchange device. (A) Cross-section (top) and top view (bottom) of the perfusion chamber. The oocyte is placed in a small cavity possessing an internal volume of 10 μl and superfused at a constant flow rate of ≈200 μl/s through a glass-capillary of 1.2-mm internal diameter connected with a manifold (not depicted) that is fixed by a micromanipulator. Bath solution exceeding the internal volume of the cavity is removed with a diaphragm pump through a glass-capillary mounted close to the chamber cavity. Two Ag/AgCl pellets are used for grounding the bath and as reference for the intracellular voltage electrode, respectively. (B) The onset of muscle type nAChR currents was used to assess the speed of solution exchange. Shown are seven superimposed current traces elicited repetitively in 1-min intervals by 5-s 30 μM acetylcholine pulses. A current rise time $t_{10–90\%}$ of ~150 ms was determined for a 10–90% increase of the current amplitude.

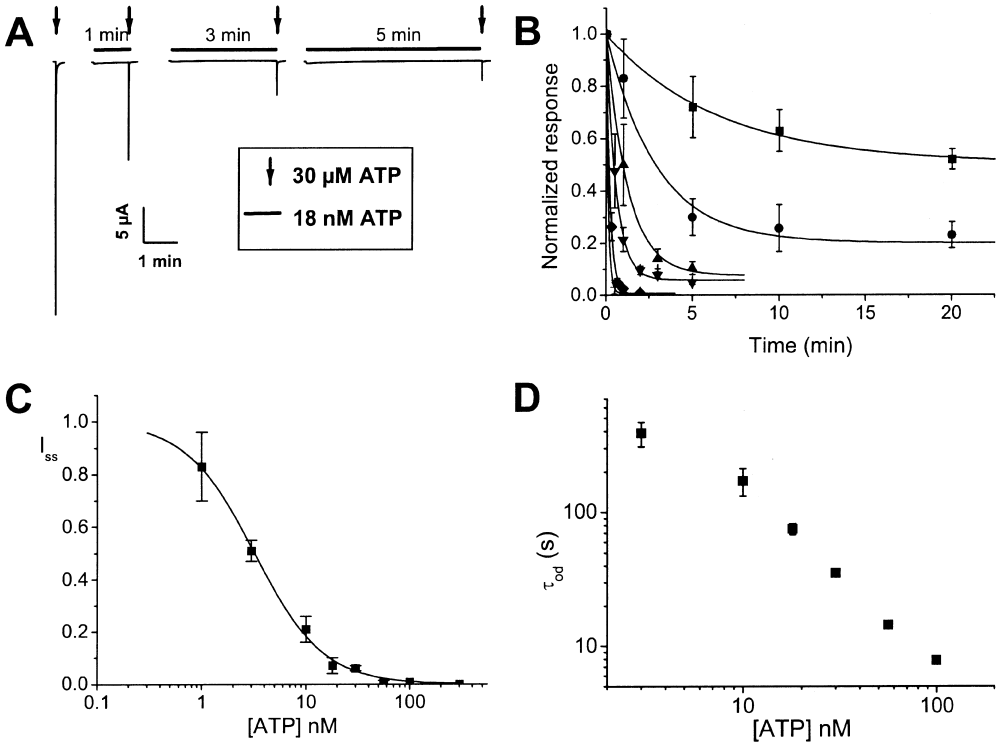

FIGURE 2. Desensitization of the $P2X_1$ receptor by incubation at submicromolar ATP concentrations. (A) Shown are current traces elicited by saturating test pulses of 30 µM ATP after preincubation of individual oocytes at 18 nM ATP for the indicated time period. (B) Rate of entry into the desensitized receptor state by preincubation in ATP-containing Mg-ORI. Desensitization was induced using 3 (■), 10 (●), 18 (▲), 30 (▼), 56 (◆), and 100 nM ATP (+). The lines represent fits of a monoexponential function to the data (6–18 determinations per data point). (C) ATP concentration dependence of steady-state desensitization. Steady-state desensitization levels represented by I_{ss} values were derived from the exponential fits of (B). The curve represents a nonlinear fit of the Hill equation to the data ($K_{1/2}$ = 3.2 ± 0.1 nM, n = 1.24 ± 0.06; 6–13 determinations per data point). The value at 1 nM ATP was obtained by preincubating the oocytes for 2 h at 1 nM ATP in a Petri dish before transferring them to the superfusion chamber, where the residual current response was elicited by the 30 µM ATP test pulse. (D) ATP concentration dependence of τ_{od}, the time-constant of onset of desensitization. τ_{od} values are derived from the nonlinear fits shown in (B).

point, the solution was switched to 30 µM ATP to elicit the residual peak current response by activating all the $P2X_1$ receptors still present in the nondesensitized state C. Fig. 2 A shows as an example of such an experiment the individual current traces of oocytes, which were first superfused for 1, 3, or 5 min with 18 nM ATP in Mg-ORi and then challenged with a test pulse of 30 µM ATP for peak current determination. To avoid any bias by incomplete recovery between repetitive applications of ATP as a result of to the long-lived desensitization, every oocyte was used only once for (residual) peak current determination by 30 µM ATP and discarded thereafter. By referring to the control response to 30 µM ATP of oocytes superfused solely with ATP-free Mg-ORi, it follows that the fraction of $P2X_1$ receptors in the desensitized state increased with time, such that after 5 min of exposure to 18 nM ATP only 10% of the maximum current response was left.

It is important to note that the term "desensitization" as used in the present study refers to both (a) the decay of the transient receptor current in presence of ATP, and (b) the rate of entry of $P2X_1$ receptors into the desensitized state by preincubation in low ATP. To distinguish kinetically between the two phenomena, we use the time constants τ_{des} and τ_{od} to characterize the rate of current decay (a) and the onset rate of desensitization (b), respectively. The time courses of onset of $P2X_1$ receptor desensitization at 3–100 nM ATP in the superfusion bath are illustrated in Fig. 2 B. To account for variable expression levels between different oocyte batches, residual peak currents elicited by 30 µM ATP after various length of perfusion with Mg-ORi with low ATP were normalized to peak currents elicited by 30 µM ATP in a subgroup of the same cRNA-injected oocytes, which were never exposed to ATP before applying the 30 µM ATP test pulse (control group). In a total of 13 control subgroups that were analyzed during the course of this study, the average current elicited by 30 µM ATP without preincubation amounted to 23.6 ± 2.1 µA; the average standard error of the measurements within the individual subgroups was 13.7 ± 2%. The normalized residual current responses were plotted for each of the various ATP concentrations versus time and the following monoexponential equation was fitted to the data

$$I_t = I_{max}\exp(-t/\tau_{od}) + I_{ss},$$

where τ_{od} signifies the time constant of onset of desensitization; I_t is the amplitude of the residual peak current response after preincubation time period t, and I_{ss} is the amplitude of the residual peak current at the

steady-state level of desensitization attained in the continuous presence of ATP. This steady-state level of desensitization is attained when the rate at which $P2X_1$ receptors enter the desensitized state equals the rate at which $P2X_1$ receptors recover from the desensitized state in the continuous presence of the respective ATP concentration. With increasing ATP concentrations in the superfusion bath, both the rate of onset of desensitization and the steady-state level of desensitization increased.

To determine the ATP dependence of this process, steady-state desensitization levels represented by I_{ss} values derived from exponential fits (Fig. 2 B) were plotted against the respective ATP concentration (Fig. 2 C). Fitting the Hill equation to the data yielded an $K_{1/2}$ value of 3.2 ± 0.1 nM. The Hill coefficient of 1.24 ± 0.06 suggests that more than one ATP molecule must bind to desensitize the receptor. The use of the Hill equation is based on the assumption that the kinetic behavior of the $P2X_1$ receptor can be described by a cyclic pseudo three-state model with *C* (closed or resting state), *O* (open state), and *D* (desensitized state) (Reaction diagram 1),

$$C + ATP \underset{k_{-1}}{\overset{k_{act}}{\leftrightarrow}} O_{ATP} \underset{k_{-2}}{\overset{k_{des}}{\leftrightarrow}} D_{ATP} \underset{k_{-3}}{\overset{k_{+3}}{\leftrightarrow}} ...C + ATP$$

Potentially existing additional conformational transitions between states *D* and *C* are combined to the rate constants k_{+3} and k_{-3}. The residual current at the end of the preincubation is proportional to the steady-state occupancy of C, which can be written as

$$C = E_{tot}/\{1 + ([ATP]/K_{1/2})^n\},$$

where E_{tot} signifies the totalized occupancies of *C*, *O*, and *D*; $K_{1/2}$ encompasses all six rate constants of the kinetic model:

$$K_{1/2} = \frac{k_{-1}k_{+3} + k_{des}k_{+3} + k_{-1}k_{-2}}{k_{act}(k_{-2} + k_{des} + k_{+3}) + k_{-3}(k_{-1} + k_{-2} + k_{des})}. \quad (1)$$

It is apparent from Fig. 2 B that the onset time constant of desensitization τ_{od} decreased with increasing ATP concentrations. The relationship between τ_{od} and the ATP concentrations is shown in Fig. 2 D.

Time Course of Recovery from Desensitization

In the previous paragraph we showed that nanomolar ATP concentrations cause profound desensitization on a slow time scale. The half-maximum steady-state desensitization occurred at 3.2 ± 0.13 nM ATP, at 3 nM ATP steady-state desensitization developed with the time constant τ = 6.5 min. As a proof for the steady-state criterion, it should be expected that recovery from desensitization occurs at a time scale similar to the development of desensitization at 3 nM ATP. To determine the recovery time course we used a protocol where 200 nM ATP was repetitively applied for a duration of 60 s in intervals ranging from 1 to 60 min. Between ATP applications oocytes were washed in ATP-free Mg-ORI. One minute after each of these ATP applications generating the current responses of interest, a control response to 200 nM ATP was elicited followed by a second one again after 1 min in ATP-free Mg-ORI. The first control response was used to normalize the preceding response of interest, the second one served for the confirmation of the first control. Fig. 3 shows the result of the recovery experiments. The data could be fitted by a monoexponential function indicating that recovery from desensitization does not involve a series of conformational changes, or that only one conformational change between desensitized state D and closed state C is rate determining. The time constant of recovery amounted to τ = 11.6 ± 1.0 min which is about twice the value of the time constant for development of steady-state desensitization at 3 nM ATP. Since Eq. 1 can be reduced to:

$$K_{1/2} = \frac{k_{des}k_{+3}}{k_{act}k_{des}} = \frac{k_{+3}}{k_{act}}$$

under certain assumptions (see DISCUSSION), the factor 2 between the two time-constants can be regarded as being compatible with our simple kinetic model: At 3 nM ATP, close to the $K_{1/2}$ value for steady-state desensitization, the model predicts that k_{+3} and k_{act} are about equal. The rate constant derived from the recovery experiments is identical to k_{+3}, whereas the measured

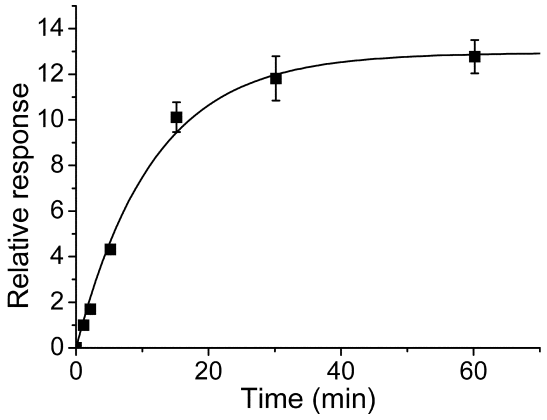

FIGURE 3. Recovery from desensitization. Test responses were elicited by 200 nM ATP applied for a duration of 60 s in intervals ranging from 1 min to 60 min. Between ATP applications oocytes were washed in ATP-free Mg-ORI. One minute after each test response, a control response to 200 nM ATP was elicited which was used to normalize the preceding response of interest. The solid line represents the fit of a monoexponential function to the data yielding the time constant τ = 11.6 ± 1.0 min (N = 4–7).

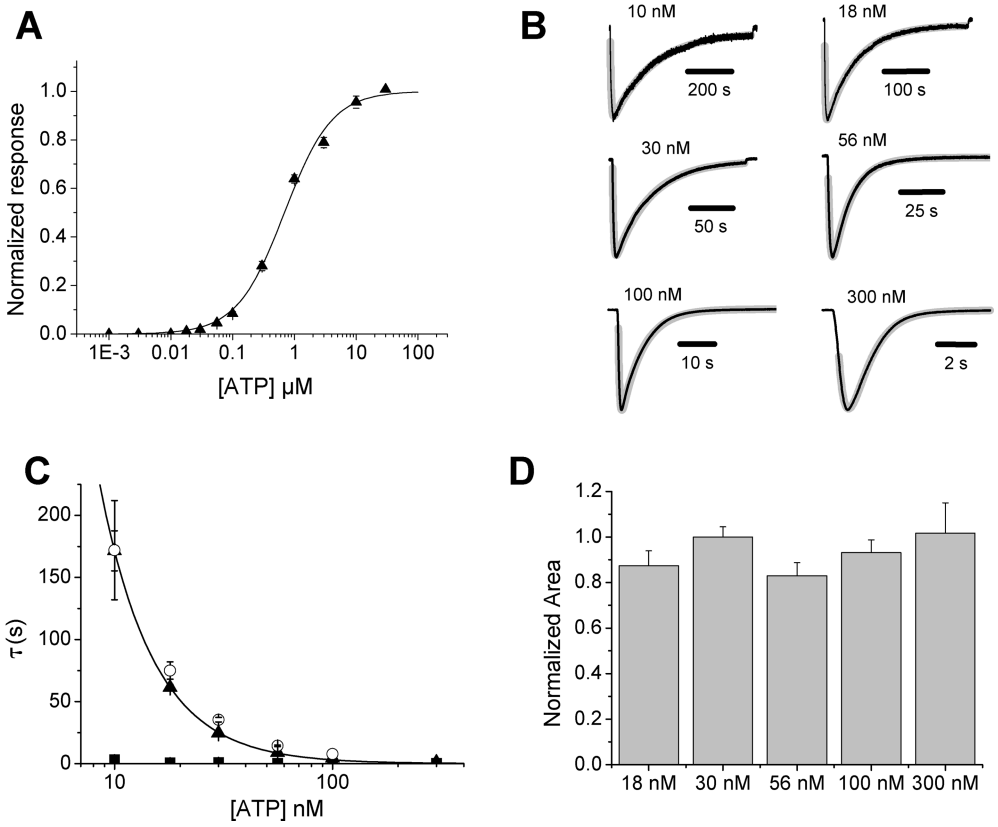

FIGURE 4. Analysis of $P2X_1$ receptor activation at submicromolar ATP concentrations. (A) ATP dose-response curve for 1 nM to 30 µM ATP (EC_{50} = 0.7 ± 0.06 µM, n = 1.13 ± 0.08; mean of 11–55 determinations per data point). (B) Scaled current traces elicited by 10–300 nM ATP. ATP was applied until the desensitization process was completed (10 min at 10 nM ATP; 10 s at 300 nM). The gray curves underlying the original current traces (in black) represent fits of the Bateman equation to the data. (C) ATP concentration dependence of activation (■) and desensitization (▲) time-constants (21–70 determinations per data point). The solid line represents a fit of equation $\tau = \tau^0[ATP]^{-n}$ to the data points (n = 1.75 ± 0.02). In addition, time constants of onset of desensitization (○) taken from Fig. 2 D were replotted to demonstrate that they follow a virtually identical ATP dependence. (D) Areas under current traces elicited by 18–300 nM ATP (11–51 determinations per column). The areas were calculated using the parameters obtained by fitting the Bateman function to the current traces in (A). Numerical integration of the receptor currents yielded virtually identical results (not depicted).

rate constant from the steady-state desensitization experiments is the sum of k_{+3} and k_{act}. This leads directly to the factor 2 between the two experimentally determined rates for development of and recovery from desensitization.

$P2X_1$ Receptor–mediated Currents Elicited by Submicromolar ATP Concentrations

Half-maximum $P2X_1$ receptor peak responses are typically observed at ATP concentrations around 1 µM. Since nanomolar ATP concentrations can effectively desensitize the $P2X_1$ receptor (compare Fig. 2), we analyzed the current responses at nanomolar ATP levels in greater detail to examine whether desensitization at low ATP involves channel opening or not. Fig. 4 A shows the dose-response curve for ATP concentrations ranging from 1 nM to 30 µM. Two different protocols were used to determine the ATP dependence of peak currents at ATP concentrations lower and higher than 100 nM, respectively. Between 100 nM and 10 µM ATP each current measurement at an ATP concentration required to establish the dose-response curve was preceded and followed by a measurement of the maximum current response to 30 µM ATP as an internal control. To this end, 5-s ATP pulses were repetitively applied in intervals of exactly 60 s. To overcome the problem that a short pulse with a low ATP concentration causes only a fraction of the total $P2X_1$ receptor pool to desensitize, a 5 s lasting pulse of 30 µM ATP was always applied immediately before the 60-s recovery period to induce all $P2X_1$ receptors to enter the desensitized state. Accordingly, no other $P2X_1$ receptors than those that recovered from the desensitized state during the 60-s recovery period were available for activation by the next test pulse of ATP. In this way, current measurements used for the dose-response curve could be normalized to the respective flanking control current responses to 30 µM ATP, thus minimizing the influence of current run-down and related phenomena on the results. At ATP concentrations between 1 and 30 nM currents are too small to be dependably resolved. Therefore, we used responses elicited directly after impaling the oocytes for determination of peak currents at these low ATP concentrations. These responses were normalized to the mean of control responses elicited by 30 µM ATP also directly after impalement. To this end, every oocyte was used only once and discarded thereafter. Despite the two different protocols used both datasets

could be combined in one plot and fitted by a single Hill equation yielding an EC_{50} value of 0.7 μM and a Hill coefficient of 1.13. For the kinetic description of the current transients, which are proportional to the occupancy of the open state, we considered the model:

$$C \xrightarrow{k_{act}} O \xrightarrow{k_{des}} D.$$

This model is deduced from Reaction diagram 1 by omitting recovery from desensitization (D → C) and backward reactions (D → O and O → C). Quantitatively, this reaction diagram can be handled by the Bateman equation, which has first been used to describe the radioactive decay of a parent element into a daughter nucleus, which itself is radioactive (Bateman, 1910).

$$I(t) = \frac{I_0 \cdot k_{act}}{k_{des} - k_{act}}[\exp(-k_{act}t) - \exp(-k_{des}t)]. \qquad (2)$$

k_{act} and k_{des} are the rate constants of receptor activation and desensitization, respectively, and I_0 is the receptor current that would be observed without receptor desensitization ($k_{des} = 0$). Fig. 4 B shows individual $P2X_1$ receptor current traces activated by application of 10–300 nM ATP. The original current traces were scaled to approximately the same size to visualize their excellent agreement with the underlying gray lines, representing the nonlinear least-squares fits of Eq. 2 to the current traces. The rate of current decay increased strongly with the ATP concentration. Plotting the time constants τ ($\tau = 1/k$) derived from the fit of the Bateman equation to the current traces versus the ATP concentration showed that the time constants of the decaying phase of the current traces are strongly ATP dependent, whereas the time constants of current onset seem to be virtually ATP independent (Fig. 4 C). The ATP dependence of the decay time constants can be adequately described by the equation $\tau = \tau^0[ATP]^{-n}$, with $n = 1.75$; τ^0 signifies the time constant at 1 nM ATP (Fig. 4 C). Fig. 4 C also shows the time constants of onset of desensitization derived from the steady-state measurements. The very similar ATP dependence of both datasets is consistent with the view that time constants of onset of desensitization and of decay of the current response both have identical kinetic origin.

It seems plausible to assign k_{act} and k_{des} of the Bateman equation to the rate constants of the rise and decay components of the current traces, respectively. However, the Bateman equation possesses the characteristic feature that the decay phase does not a priori reflect k_{des}, but rather the process, which exhibits the lowest rate constant, i.e., k_{act} or k_{des}. In other words, identically shaped current traces can be expected independent of whether receptor activation or deactivation represents the ATP concentration–dependent reaction as long as the ATP concentration–dependent step is slow compared with the other one. A discrimination between the two possibilities—ATP dependence of either k_{act} or k_{des}—can be made on basis of the consideration that an ATP concentration–dependent acceleration of the desensitization reaction would result in current peaks that decrease at increasing ATP concentrations. Since this is obviously not the case, we conclude that the decay phase reflects the rate of receptor activation rather than receptor desensitization and consequently that the desensitization reaction at low ATP occurs much faster than the activation reaction ($k_{des} >> k_{act}$). At ATP concentrations >100 nM the rate of current onset becomes faster than the desensitization rate constant k_{des} and the decay of the current is then defined by the desensitization rate constant.

Since the area under a current trace, AUC, is represented by the integral of the Bateman equation,

$$AUC = \int_0^\infty I(t) = \frac{I_0}{k_{des}},$$

the linear three-state-model predicts further that the AUC values are independent of the ATP concentration provided that the rate constant of desensitization, k_{des}, is ATP independent as concluded above. To test this prediction, the AUC values were calculated for ATP concentrations between 18 and 300 nM. Fig. 4 D shows the calculated areas normalized to the area at 30 nM ATP and demonstrates that there is indeed no obvious ATP dependence of the AUC at concentrations between 18 and 300 nM ATP. The ATP independence of the AUC values corroborates our view that the ATP dependence of the decay phases reflects the ATP dependent activation rate constant k_{act} at < 100 nM ATP.

DISCUSSION

The present study shows that the rat $P2X_1$ receptor, which requires 0.7 μM ATP for half-maximum activation, becomes profoundly desensitized in the continuous presence of ~200-fold lower ATP concentrations. Inactivation by low concentrations of a continuously present agonist has previously been observed to occur with various neurotransmitters and drugs, including serotonin (Neijt et al., 1989; Bartrup and Newberry, 1996), acetylcholine (Boyd and Cohen, 1980), and nicotine (Dani and Heinemann, 1996). For the nicotinic receptors it has been shown that this type of desensitization, which occurs without receptor activation, results from the direct binding of an agonist to a desensitized receptor state D*, which has a several hundredfold higher agonist affinity than the resting receptor state R. The high affinity, desensitized receptor pool is in equilibrium with the unliganded resting receptors, and accounts for ~20% of the nicotinic receptors in the absence of agonist (Heidmann and Changeux, 1979). Oc-

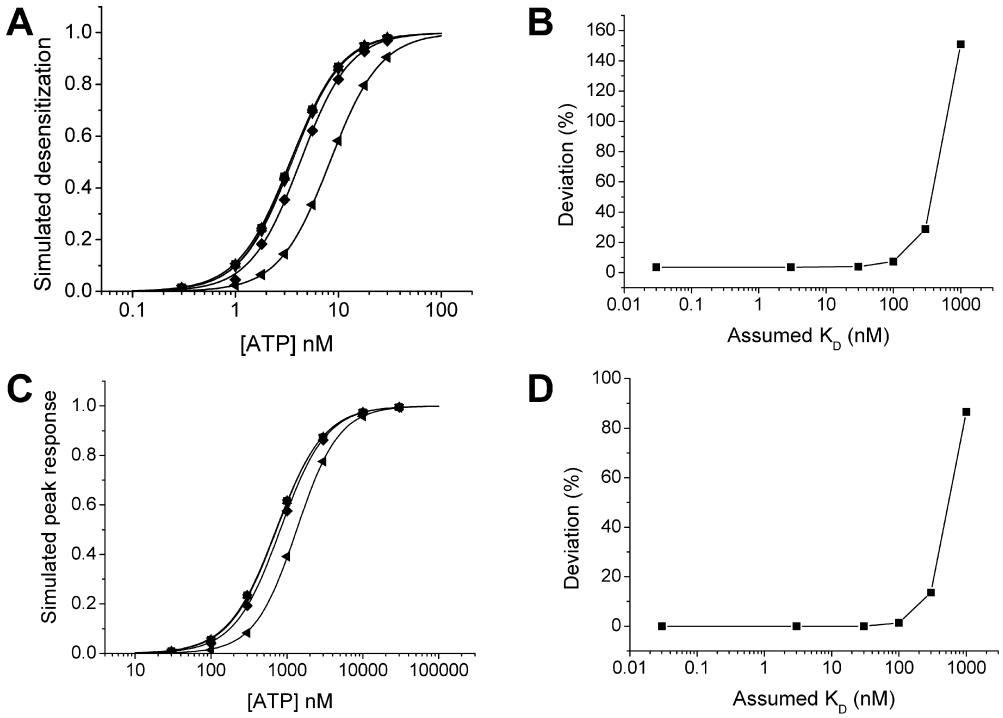

FIGURE 5. Analysis of simulated receptor currents. Receptor currents were simulated for the cyclic three-state model by using the Gepasi Software and analyzed in the same manner as the experimental data. (A) ATP dependence of simulated peak currents in dependence of assumed genuine K_D values for receptor activation of 0.03 (■), 3 (●), 30 (▲), 100 (▼), 300 (◆) and 1.000 nM (◀). A fit of the Hill equation to the simulated data yielded EC_{50} values of 0.72–1.3 μM for K_D values ranging from 0.03 to 1,000 nM, respectively. (B) Relative deviations of the calculated EC_{50} taken from A from the experimentally determined EC_{50} value in dependence of the assumed genuine K_D values. (C) Steady-state desensitization was calculated using the same set of simulated currents as in (A). A fit of the Hill equation resulted in apparent $K_{1/2}$ values of 3.4–8.3 nM for K_D values of 0.03–1,000 nM, respectively. (D) Relative deviations from the calculated $K_{1/2}$ values from the experimentally determined $K_{1/2}$ value in dependence of genuine assumed K_D values.

cupation of these high affinity sites at low agonist concentrations drives R through D* toward D*·agonist, leading to receptor desensitization without concomitant channel opening.

Steady-state Desensitization by ATP Cannot be Attributed to a High Affinity Predesensitized P2X$_1$ Receptor Pool

In obvious contrast to these results, we observe significant $P2X_1$ receptor–mediated currents at the same nanomolar concentrations of ATP, which eventually drive large fractions of the total $P2X_1$ receptor pool into a desensitized configuration, from which they recover very slowly. From the identical total areas under the current transients, we infer that the same number of receptors are activated irrespective of whether the activation occurs slowly or rapidly at low or high ATP concentrations, respectively. Current traces elicited by ATP concentrations <18 nM, which are too low to produce near-to-complete desensitization, were not included in the area evaluation to exclude a significant current contribution by $P2X_1$ receptors that recover from the desensitized state during the observation period. The important conclusion from these observations is that low ATP concentrations desensitize the $P2X_1$ receptor by binding to the resting receptor state R rather than by binding to a desensitized high affinity state D*. This conclusion is also corroborated by the finding that decay of receptor current and onset of desensitization follow the same time course. Accordingly, desensitization by nanomolar concentrations of ATP cannot be attributed to the existence of a population of high affinity predesensitized $P2X_1$ receptors, but must be inherent to other steps of the reaction pathway.

Fast Desensitization as a Determinant of Micromolar ATP Potency for Receptor Activation

But how then explain the large difference between the EC_{50} value for receptor activation and the $K_{1/2}$ value for steady-state desensitization of 0.7 μM *vs.* 3.2 nM, respectively? The EC_{50} value for $P2X_1$ receptor activation is derived from peak current measurements, which reflect ATP binding to the receptor followed by channel opening and rapid desensitization. The use of the Hill-equation to describe steady-state desensitization was based on reaction diagram 1 (see RESULTS). This scheme can be further simplified by assuming that k_{-1} and k_{-2} are negligibly small (both rate constants can be set to zero for appropriate description of receptor currents, see RESULTS). Assuming further that $k_{des} >> k_{+3}$, i.e., that desensitization occurs much faster than recovery from desensitization, and $k_{act} >> k_{-3}$, i.e., that ATP binding leads predominantly to channel opening and not directly to desensitization, the above equation reduces to

$$K_{1/2} = \frac{k_{des}k_{+3}}{k_{act}k_{des}} = \frac{k_{+3}}{k_{act}}.$$

This simplified equation can be assigned to a two-state model,

$$C + ATP \underset{k_{+3}}{\overset{k_{act}}{\leftrightarrow}} D_{ATP},$$

where k_{act} is now the apparent desensitization rate constant; k_{+3} remains the rate constant of recovery from desensitization. This signifies that steady-state desensitization is approximately determined by the activation rate constant k_{act} and the recovery rate constant k_{+3}. The validity of this simplification is strengthened by the finding, predicted by the model, that development of steady-state desensitization at 3 nM ATP occurs at a rate twice as fast as the rate of recovery from desensitization. In the cyclic three-state reaction scheme, closure of receptor state *O* occurs by both backward reaction to the closed state *C* and forward reaction to the desensitized state *D* with the dissociation rate constant for agonist unbinding k_{-1} and the desensitization rate constant k_{des}, respectively. If k_{-1} is slow compared with k_{des}, the apparent affinity of the receptor deduced from the ATP concentration–dependent magnitude of peak currents is determined by the quotient of k_{act} and k_{des}, rather than by the genuine ATP binding affinity of the receptor, which is given by k_{-1}/k_{act}. In other words, apparently as a result of the rapid rate of receptor desensitization and the comparably slow rate of ATP unbinding, peak current measurements provide a determination of the EC_{50} value under nonsteady-state conditions (Leff, 1986). Hence, the EC_{50} value of 0.7 μM does not reflect ATP binding equilibrium, since virtually all activated $P2X_1$ receptors close by a $O \rightarrow D$ transition rather than by a $O \rightarrow C$ transition.

The view that $k_{des} >> k_{-1}$ is supported by model calculations showing that the characteristics of steady-state desensitization as well as receptor currents can be adequately described by a reaction model, in which the dissociation rate constant k_{-1} is set to zero. Using the experimentally determined values for k_{act} and k_{+3}, with k_{-1}, k_{-2}, and k_{-3} set to zero, simulated receptor currents were generated with the Gepasi software for the cyclic three-state reaction model. By analyzing these data in the same way as the experimental data, $K_{1/2}$ values were obtained that amounted to 0.7 μM and 3.2 nM for ATP-dependent current activation and steady-state desensitization, respectively, which are identical to the experimentally determined values (Fig. 5, A and C).

The High ATP Affinity for Steady-state $P2X_1$ Receptor Desensitization Is Predominantly Determined by Fast Desensitization Combined with Extremely Slow Recovery

While these considerations illuminate the low ATP potency for $P2X_1$ receptor activation and corroborate that our models can predict the distinct $K_{1/2}$ values, it remains unclear which reaction step is responsible for the 3.2 nM affinity of steady-state desensitization. A possible candidate for a high ATP affinity is the resting state C itself. However, the genuine ATP affinity of state C cannot be directly deduced from our models, since the Bateman equation solely provides an estimate of the on rate constant k_{act}, whereas the off rate constant k_{-1} is considered to be negligibly low in our reaction models on the basis of $k_{-1} << k_{des}$. To provide a rough estimate of the upper limit of the dissociation rate constant k_{-1}, we generated numerically simulated receptor currents using again the experimentally determined rate constants, with the sole exception that k_{-1} was not set to zero, but varied to produce genuine K_D values (equal to k_{-1}/k_{act}) of 10^{-2} to 10^3 nM. The resulting ATP-dependent currents were analyzed in the same way as the experimental data. Fig. 5, A and C, shows the dose-response curves for simulated receptor activation and steady-state desensitization in dependence of the chosen genuine K_D values for ATP. Fig. 5, B and D, depicts the relative deviations of the simulated EC_{50} values for activation and the $K_{1/2}$ value for steady-state desensitization from the experimentally determined values (0.7 μM and 3.2 nM, respectively). In both cases significant deviation from the experimental data occurs at K_D >100 nM. Below 100 nM ATP, the values for both activation and steady-state desensitization were found to be virtually independent of the intrinsic ATP binding affinity of the $P2X_1$ receptor. From these model calculations, we conclude that the intrinsic ATP affinity of the $P2X_1$ receptor must be <100 nM; therefore, an intrinsic ATP affinity in the low nanomolar range is neither excluded nor supported by our data. In any case, the low $K_{1/2}$ value of 3.2 nM for steady-state $P2X_1$ receptor desensitization is related to the extremely slow recovery of the $P2X_1$ receptor from the desensitized state such that the apparent affinity approximates k_{+3}/k_{act}. It is interesting to note that a binding affinity in the nanomolar range has been observed in tissues expressing native P2X receptors in early radiotracer binding experiments using the agonists [^{35}S]ATP and [^{3}H]αβ-methylene ATP as ligands (Bo and Burnstock, 1990; Michel and Humphrey, 1993). If recovery from desensitization is rate limited by agonist dissociation rather than an agonist-independent conformational change, the $K_{1/2}$ value for steady-state desensitization of our study and the binding affinity found in the radiotracer experiments could have the same physical origin.

It has been shown that $P2X_1$ receptor channels have a single-channel conductance of ~19 pS and that openings occur in brief flickery bursts (Evans, 1996). This flickery behavior is not considered by our simple kinetic model, but can easily be introduced by the addition of an explicit opening reaction by inserting a closed ATP-liganded state between C and O. Another feature at the single-channel level is that P2X receptors

continuously exposed to ATP reopen after longer periods of closure. This reopening is already supported by our model in the present form, in which recovery from desensitization occurs on a slow time-scale without channel opening.

Altogether, our data indicate that the kinetic behavior of the $P2X_1$ receptor resembles in several aspects that of LGIC of the nicotinic superfamily, including its high sensitivity to low concentrations of continuously present agonist, which drive large fractions of the receptor into a desensitized state. However, the underlying mechanism that accounts for desensitization at low agonist concentrations seems to be fundamentally different. The high sensitivity of nicotinic receptors to desensitization by a continuously present agonist results from the existence of a significant fraction of the receptor in a high affinity desensitized state, which is in equilibrium with the resting state, and to which the agonist binds without opening the channel. In contrast, the $P2X_1$ receptor must first open to desensitize even at low ATP concentrations, indicating that an unliganded high-affinity desensitized $P2X_1$ receptor state D* does not contribute significantly to the desensitization process at the examined ATP concentrations. The apparent ATP affinities for channel activation and steady-state desensitization are predominantly determined by receptor desensitization and recovery from desensitization, respectively, in both cases in combination with receptor activation. The rapid rate of receptor desensitization results in an apparent ATP affinity in the 0.7 μM range, whereas the extremely slow recovery from the desensitized state leads to a 200-fold higher apparent affinity for continuously present ATP causing steady-state desensitization. Our model calculations indicate that the resting $P2X_1$ receptor possesses an intrinsic ATP affinity of $<$100 nM. Up to this concentration, the intrinsic ATP affinity seems to have no influence on the $K_{1/2}$ values for receptor activation and desensitization.

Since these different effects of ATP on the $P2X_1$ receptor are separated by more than two orders of magnitude, desensitization can be fully developed before current activation becomes significant. The extent to which synaptic transmission is physiologically limited by P2X receptor desensitization is not clear. However, since significant extracellular ATP concentrations are attained under a variety of physiological and pathophysiological conditions such as ischemic tissue damage (Rathbone et al., 1999), the long-lasting refractory closed state suggests that $P2X_1$ receptor responses can be obscured in vivo by unexpectedly low concentrations of ATP.

This work was supported by grants of the Deutsche Forschungsgemeinschaft (Schm536/2-3, Schm536/2-4, and GRK137-2) and the Pfleger Foundation.

Olaf S. Andersen served as editor.

Submitted: 22 October 2002
Revised: 27 March 2003
Accepted: 27 March 2003

REFERENCES

Bartrup, J.T., and N.R. Newberry. 1996. Electrophysiological consequences of ligand binding to the desensitized 5-HT_3 receptor in mammalian NG108-15 cells. *J. Physiol.* 490:679–690.

Bateman, H. 1910. The solution of a system of differential equations occurring in the theory of radioactive transformations. *Proc. Cambridge Phil. Soc.* 16:423–427.

Bo, X.N., and G. Burnstock. 1990. High- and low-affinity binding sites for [^{3}H]-α, β-methylene ATP in rat urinary bladder membranes. *Br. J. Pharmacol.* 101:291–296.

Bo, X.N., Y. Zhang, M. Nassar, G. Burnstock, and R. Schoepfer. 1995. A P2X purinoceptor cDNA conferring a novel pharmacological profile. *FEBS Lett.* 375:129–133.

Boue-Grabot, E., V. Archambault, and P. Seguela. 2000. A protein kinase C site highly conserved in P2X subunits controls the desensitization kinetics of $P2X_2$ ATP-gated channels. *J. Biol. Chem.* 275:10190–10195.

Boyd, N.D., and J.B. Cohen. 1980. Kinetics of binding of [^{3}H]acetylcholine to Torpedo postsynaptic membranes: association and dissociation rate constants by rapid mixing and ultrafiltration. *Biochemistry.* 19:5353–5358.

Brake, A.J., M.J. Wagenbach, and D. Julius. 1994. New structural motif for ligand-gated ion channels defined by an ionotropic ATP receptor. *Nature.* 371:519–523.

Buell, G., C. Lewis, G. Collo, R.A. North, and A. Surprenant. 1996. An antagonist-insensitive P2X receptor expressed in epithelia and brain. *EMBO J.* 15:55–62.

Burnstock, G. 1999. Current status of purinergic signalling in the nervous system. *Prog. Brain Res.* 120:3–10.

Changeux, J.P. 1990. The TiPS lecture. The nicotinic acetylcholine receptor: an allosteric protein prototype of ligand-gated ion channels. *Trends Pharmacol. Sci.* 11:485–492.

Chen, C.C., A.N. Akopian, L. Sivilotti, D. Colquhoun, G. Burnstock, and J.N. Wood. 1995. A P2X purinoceptor expressed by a subset of sensory neurons. *Nature.* 377:428–431.

Collo, G., R.A. North, E. Kawashima, E. Merlo-Pich, S. Neidhart, A. Surprenant, and G. Buell. 1996. Cloning of $P2X_5$ and $P2X_6$ receptors and the distribution and properties of an extended family of ATP-gated ion channels. *J. Neurosci.* 16:2495–2507.

Costa, A.C., J.W. Patrick, and J.A. Dani. 1994. Improved technique for studying ion channels expressed in Xenopus oocytes, including fast superfusion. *Biophys. J.* 67:395–401.

Dani, J.A., and S. Heinemann. 1996. Molecular and cellular aspects of nicotine abuse. *Neuron.* 16:905–908.

Dilger, J.P., and R.S. Brett. 1990. Direct measurement of the concentration- and time-dependent open probability of the nicotinic acetylcholine receptor channel. *Biophys. J.* 57:723–731.

Ennion, S.J., and R.J. Evans. 2001. Agonist-stimulated internalisation of the ligand-gated ion channel $P2X_1$ in rat vas deferens. *FEBS Lett.* 489:154–158.

Evans, R.J. 1996. Single channel properties of ATP-gated cation channels (P2X receptors) heterologously expressed in Chinese hamster ovary cells. *Neurosci. Lett.* 212:212–214.

Heidmann, T., and J.P. Changeux. 1979. Fast kinetic studies on the interaction of a fluorescent agonist with the membrane-bound acetylcholine receptor from *Torpedo marmorata*. *Eur. J. Biochem.* 94: 255–279.

Katz, B., and S. Thesleff. 1957. A study of the 'desensitization' produced by acetylcholine at the motor end-plate. *J. Physiol.* 138:63–

80.

Koshimizu, T., M. Koshimizu, and S.S. Stojilkovic. 1999. Contributions of the C-terminal domain to the control of P2X receptor desensitization. *J. Biol. Chem.* 274:37651–37657.

Leff, P. 1986. Potential errors in agonist dissociation constant estimation caused by desensitization. *J. Theor. Biol.* 121:221–232.

Mackenzie, A.B., A. Surprenant, and R.A. North. 1999. Functional and molecular diversity of purinergic ion channel receptors. *Ann. NY Acad. Sci.* 868:716–729.

Mendes, P. 1993. GEPASI: a software package for modelling the dynamics, steady states and control of biochemical and other systems. *Comput. Appl. Biosci.* 9:563–571.

Mendes, P. 1997. Biochemistry by numbers: simulation of biochemical pathways with Gepasi 3. *Trends Biochem. Sci.* 22:361–363.

Methfessel, C., V. Witzemann, T. Takahashi, M. Mishina, S. Numa, and B. Sakmann. 1986. Patch clamp measurements on *Xenopus laevis* oocytes: currents through endogenous channels and implanted acetylcholine receptor and sodium channels. *Pflugers Arch.* 407:577–588.

Michel, A.D., and P.P. Humphrey. 1993. Distribution and characterisation of [^{3}H]α,β-methylene ATP binding sites in the rat. *Naunyn Schmiedebergs Arch. Pharmacol.* 348:608–617.

Neijt, H.C., J.J. Plomp, and H.P. Vijverberg. 1989. Kinetics of the membrane current mediated by serotonin 5-HT_3 receptors in cultured mouse neuroblastoma cells. *J. Physiol.* 411:257–269.

Nicke, A., H.G. Bäumert, J. Rettinger, A. Eichele, G. Lambrecht, E. Mutschler, and G. Schmalzing. 1998. $P2X_1$ and $P2X_3$ receptors form stable trimers: a novel structural motif of ligand-gated ion channels. *EMBO J.* 17:3016–3028.

Nicke, A., C. Büttner, A. Eichele, G. Lambrecht, and G. Schmalzing. 1999a. Evolving view of quaternary structures of ligand-gated ion channels. *Prog. Brain Res.* 120:61–80.

Nicke, A., J. Rettinger, E. Mutschler, and G. Schmalzing. 1999b. Blue native PAGE as a useful method for the analysis of the assembly of distinct combinations of nicotinic acetylcholine receptor subunits. *J. Recept. Signal Transduct. Res.* 19:493–507.

Nicke, A., J. Rettinger, and G. Schmalzing. 2003. Monomeric and dimeric byproducts are the principal functional elements of higher order $P2X_1$ concatamers. *Mol. Pharmacol.* 63:243–252.

North, R.A. 1996. P2X receptors: a third major class of ligand-gated ion channels. *Ciba Found. Symp.* 198:91–105.

Rathbone, M.P., P.J. Middlemiss, J.W. Gysbers, C. Andrew, M.A. Herman, J.K. Reed, R. Ciccarelli, P. Di Iorio, and F. Caciagli. 1999. Trophic effects of purines in neurons and glial cells. *Prog. Neurobiol.* 59:663–690.

Rettinger, J., A. Aschrafi, and G. Schmalzing. 2000. Roles of individual *N*-glycans for ATP potency and expression of the rat $P2X_1$ receptor. *J. Biol. Chem.* 275:33542–33547.

Schmalzing, G., S. Gloor, H. Omay, S. Kröner, H. Appelhans, and W. Schwarz. 1991. Up-regulation of sodium pump activity in *Xenopus laevis* oocytes by expression of heterologous β1 subunits of the sodium pump. *Biochem. J.* 279:329–336.

Soto, F., M. Garcia-Guzman, and W. Stühmer. 1997. Cloned ligand-gated channels activated by extracellular ATP (P2X receptors). *J. Membr. Biol.* 160:91–100.

Stoop, R., S. Thomas, F. Rassendren, E. Kawashima, G. Buell, A. Surprenant, and R.A. North. 1999. Contribution of individual subunits to the multimeric $P2X_2$ receptor: estimates based on methanethiosulfonate block at T336C. *Mol. Pharmacol.* 56:973–981.

Surprenant, A., F. Rassendren, E. Kawashima, R.A. North, and G. Buell. 1996. The cytolytic P_{2Z} receptor for extracellular ATP identified as a P_{2X} receptor ($P2X_7$). *Science.* 272:735–738.

Valera, S., N. Hussy, R.J. Evans, N. Adami, R.A. North, A. Surprenant, and G. Buell. 1994. A new class of ligand-gated ion channel defined by P_{2x} receptor for extracellular ATP. *Nature.* 371:516–519.

Werner, P., E.P. Seward, G.N. Buell, and R.A. North. 1996. Domains of P2X receptors involved in desensitization. *Proc. Natl. Acad. Sci. USA.* 93:15485–15490.

Witzemann, V., E. Stein, B. Barg, T. Konno, M. Koenen, W. Kues, M. Criado, M. Hofmann, and B. Sakmann. 1990. Primary structure and functional expression of the α-, β-, γ-, δ- and ε-subunits of the acetylcholine receptor from rat muscle. *Eur. J. Biochem.* 194:437–448.